Nucleic Acids Research, 2001, Vol. 29, No. 13 **e62**

Exciton interaction in molecular beacons: a sensitive sensor for short range modifications of the nucleic acid structure

Serena Bernacchi and Yves Mély*

Laboratoire de Pharmacologie et Physico-Chimie des Interactions Cellulaires et Moléculaires, UMR 7034 CNRS, Faculté de Pharmacie, Université Louis Pasteur, 74 Route du Rhin, 67401 Illkirch Cedex, France

Received February 19, 2001; Revised and Accepted May 8, 2001

ABSTRACT

Molecular beacons are hairpin-shaped, single-stranded oligonucleotides constituting sensitive fluorescent DNA probes widely used to report the presence of specific nucleic acids. In its closed form the stem of the hairpin holds the fluorophore covalently attached to one end, close to the quencher, which is covalently attached to the other end. Here we report that in the closed form the fluorophore and the quencher form a ground state intramolecular heterodimer whose spectral properties can be described by exciton theory. Formation of the heterodimers was found to be poorly sensitive to the stem sequence, the respective positions of the dyes and the nature of the nucleic acid (DNA or RNA). The heterodimer allows strong coupling between the transition dipoles of the two chromophores, leading to dramatic changes in the absorption spectrum that are not compatible with a Förster-type fluorescence resonance energy transfer (FRET) mechanism. The excitonic heterodimer and its associated absorption spectrum are extremely sensitive to the orientation of and distance between the dyes. Accordingly, the application of molecular beacons can be extended to monitoring short range modifications of the stem structure. Moreover, the excitonic interaction was also found to operate for doubly end-labeled duplexes.

INTRODUCTION

Molecular beacons represent a new class of DNA probes that correspond to single-stranded oligonucleotides possessing a stem–loop structure (1). The loop portion is usually a probe sequence that is complementary to the sequence of a target nucleic acid. The stem is formed by the annealing of two complementary arm sequences located on either side of the loop sequence. A fluorophore moiety is attached to the end of one arm and a non-fluorescent quencher (usually DABCYL) is attached to the end of the other arm. The two moieties are held close together, causing the fluorescence of the fluorophore to be highly quenched. In contrast, hybridization of the molecular beacons with sequences complementary to their loop sequences causes an opening of the stem that moves the fluorophore and the quencher away from each other and thus restores the fluorescence of the fluorophore. Due to the high sensitivity of fluorescence techniques, molecular beacons constitute a powerful tool to report the presence of a specific complementary nucleic acid. They have been used for monitoring PCR (2), real-time detection of DNA–RNA hybridization in living cells (3), DNA mutation analysis (4), development of ultrasensitive DNA sensors (5), detection of pathogenic viruses (6) and protein–DNA interactions (7).

The weak fluorescence of molecular beacons in the closed form is thought to be due to a Förster-type fluorescence resonance energy transfer (FRET) mechanism that permits a radiationless transfer of electronic excitation energy from the donor (fluorophore) to the acceptor (quencher) molecule (1). However, in order for FRET to operate, a very weak dipolar coupling between the donor and acceptor is required (8–10). Fulfillment of this condition in molecular beacons is not obvious due to the short distances between the two covalently bound dyes at the 5′ and 3′ positions. In this context, the aim of this work was to further investigate the mechanism of transfer of electronic excitation energy between the two covalently linked dyes. Using absorption and fluorescence techniques we here report the existence of strong intramolecular dipole–dipole coupling that can be described by exciton theory (10–12). This theory relies on formation of an intramolecular ground state heterodimer between the two dyes that allows strong coupling between their transition dipoles. This causes delocalization of excitation over the two dyes and leads to large changes in the absorption spectrum. Since coupling strongly depends on the exact geometry of and distance between the dyes, the associated spectral changes can be used to investigate short range modifications of the molecular beacon stem structure.

MATERIALS AND METHODS

Materials

Double-labeled, single-labeled and non-labeled DNA and RNA sequences were synthesized on the 0.2 µmol scale by IBA GmbH Nucleic Acids Product Supply (Göttingen,

*To whom correspondence should be addressed. Tel: +33 3 90 24 42 63; Fax: +33 3 90 24 43 12; Email: mely@pharma.u-strasbg.fr

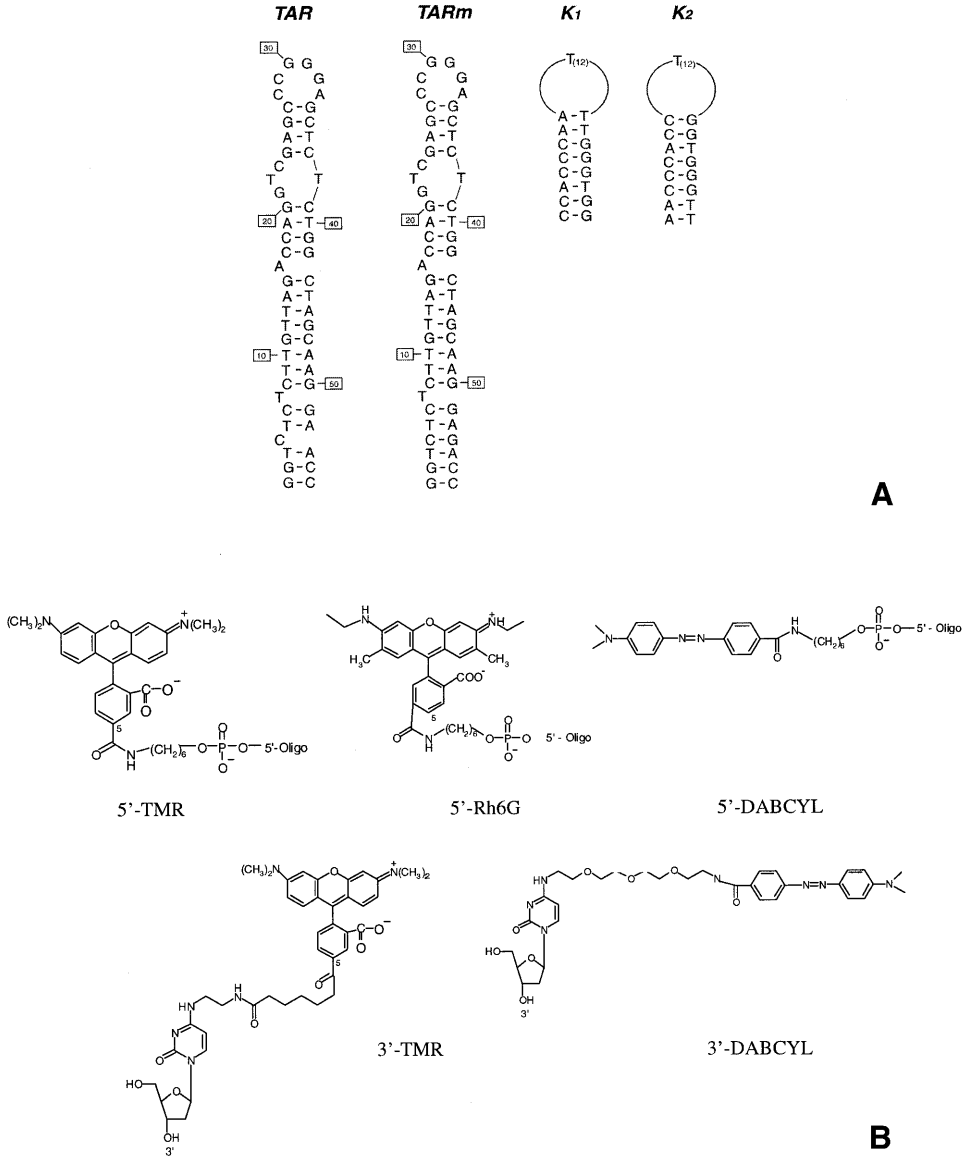

Figure 1. Oligonucleotide sequences (**A**) and chemical structures of the dyes and linkers (**B**) used in the present study.

Germany). The 5′-terminus of the oligonucleotides used in this study (Fig. 1A) was labeled with either carboxytetramethylrhodamine (TMR), 4-(4′-dimethylaminophenylazo) benzoic acid (DABCYL) or 6-carboxyrhodamine 6G (Rh6G) via an amino linker with a six carbon spacer arm (Fig 1B). The 3′-terminus of the oligonucleotides was labeled with either TMR using the same procedure or DABCYL using a special solid support with the dye already attached. Double-labeled sequences were purified by the manufacturer by reverse phase HPLC and polyacrylamide gel electrophoresis. The purity of the labeled oligonucleotides was checked by electrospray ionization mass spectrometry (13) and found to be >93%. Experiments were performed in 25 mM Tris–HCl, pH 7.5, 30 mM NaCl and 0.2 mM $MgCl_2$. Hybridization assays were performed by mixing 10 nM labeled TARm with 15 nM complementary sequence in the same buffer as above, except that 1 M NaCl was added. The mixture was heated to 85°C for 2.5 min, then stepwise cooled to 0°C.

Spectrophotometric measurements

Absorption spectra were recorded on a Cary 4 spectrophotometer, thermostated with a circulating water bath. Oligonucleotide concentrations (expressed in strands) were calculated at 260 nm using extinction coefficients of 521.900, 369.600 and 244.100 M^{-1} cm^{-1} for the DNA and RNA forms of TARm and the K1 and K2 sequences, respectively.

Melting curves were recorded by following the temperature dependence of the absorbance changes at the indicated wavelengths. The temperature was measured inside the cell with a thermocouple inserted in the cell. The melting curves were fitted assuming a two-state model (14) by:

$$A = \{A_{min} + A_{max} \exp[-\Delta H°/R(1/T - 1/T_m)]\}/ \{1 + \exp[-\Delta H°/R(1/T - 1/T_m)]\} \quad \mathbf{1}$$

where A_{min} and A_{max} are the absorbance of the native and melted oligonucleotides, respectively, T_m is the melting

temperature, ΔH° is the enthalpy change and R is the gas constant. Fluorescence excitation and emission spectra were recorded at 20.0 ± 0.5°C on an SLM 48000 spectrofluorometer. The excitation and emission bandwidths were 4 and 8 nm, respectively.

The fluorescence lifetimes of the sequences labeled with TMR were measured by the phase and modulation method on an SLM48000 spectrofluorometer. The excitation wavelength was set at 518 nm and the emission was collected through a 550 nm high band pass Kodak filter. The modulation frequencies of the excitation light ranged from 5 to 90 MHz. Data analysis was performed using the SLM software. Rh6G in methanol (τ = 3.9 ns) was taken as a reference (15).

RESULTS

Evidence of exciton interaction

In the present study we first used a molecular beacon with a deoxyribonucleic sequence corresponding to the transactivation response region (TAR) of the HIV-1 MAL strain. The 55 nt long TAR (Fig. 1A) is part of the HIV long terminal repeat duplicated at the 5′- and 3′-end of the viral RNA and forms a stable hairpin structure (16). During the virus life cycle this sequence exists in both RNA and DNA forms and plays a critical role in the regulation of transcription efficiency (17–19), packaging of genomic RNA (20) and the first strand transfer reaction during reverse transcription (21,22). Since the secondary structure of TAR shows a bulge loop (composed of a C residue) at position 4, which may not optimally stabilize the dye pair in the molecular beacon, the 3′-terminal $_{53}ACC_{55}$ sequence was replaced by GACC. This removes the bulge loop and induces the formation of a 6 bp stem (Fig. 1A) that is optimal for keeping the dyes close together (1,23). The mutated sequence was called TARm. Though this sequence differs somewhat from the sequences usually found in molecular beacons, its use is reasonable since TAR has been shown to readily hybridize with its complementary sequence under mild conditions (21,22).

As a first step we investigated the spectroscopic properties of TMR–5′-TARm-3′–DABCYL, a molecular beacon where TARm is 5′-labeled with TMR and 3′-labeled with DABCYL. The absorption spectrum of this molecular beacon clearly differed from the spectrum of an equimolecular mixture of TARm 5′-labeled with TMR (TMR–5′-TARm) and TARm 3′-labeled with DABCYL (TARm-3′–DABCYL) (Fig. 2A). The main differences are a shift in the absorption maximum to the red by 3 nm and a strong decrease in the absorbance of the TMR peak by 35%. Moreover, the absorption peak of DABCYL, which is hardly visible in an equimolecular mixture of TMR–5′-TARm and TARm-3′–DABCYL, is strongly increased in TMR–5′-TARm-3′–DABCYL and shows a clear peak at 486 nm. These dramatic changes in the absorption spectra are clearly incompatible with a Förster-type FRET mechanism, since the weak dipolar coupling that governs this mechanism does not induce any change in the absorption spectrum (10). In contrast, these spectral changes are similar to those previously described in doubly-labeled protease substrates (24,25) and thus may be described by the molecular exciton model. This model relies on the formation of an intramolecular ground state heterodimer between the two dyes.

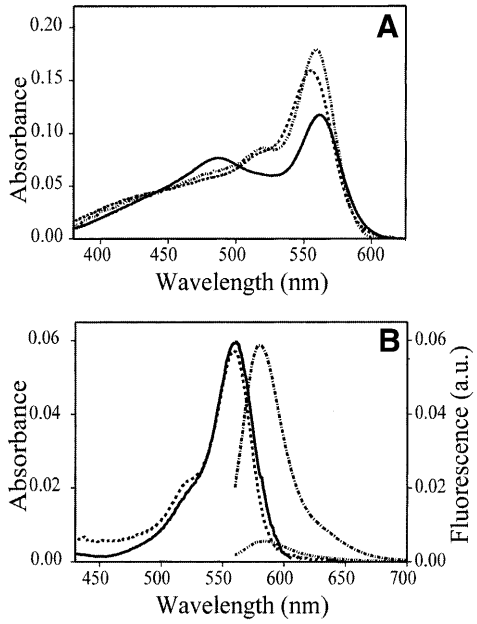

Figure 2. Spectral properties of TMR–5′-TARm-3′–DABCYL. (**A**) Absorption spectra of TMR–5′-TARm-3′–DABCYL at 20 (solid line) and 65°C (dashed line). The absorption spectrum (dash-dot-dot-dashed line) of an equimolecular mixture of TMR–5′-TARm and TARm-3′–DABCYL was recorded at 20°C. (**B**) Excitation and emission spectrum of TMR–5′-TARm-3′–DABCYL. The excitation spectrum of TMR–5′-TARm-3′–DABCYL (dashed line) was recorded at an emission wavelength of 580 nm. The emission spectrum of TMR–5′-TARm-3′–DABCYL (dash-dot-dot-dashed line) and TMR–5′-TARm (dash-dotted line) were recorded at an excitation wavelength of 550 nm. The solid line corresponds to the absorption spectrum of TMR–5′-TARm.

This allows strong coupling between the transition dipoles of the two dyes, which causes delocalization of excitation over the two dyes (10–12). It follows that the spectral properties can no longer be ascribed to the individual dyes but correspond to a unique optical signature of the heterodimer. Furthermore, the increase in the DABCYL absorption band and the concomitant decrease in the TMR band are typical of an H-type geometry, in which the transition dipoles of the individual chromophores are parallel to each other and normal to the radius vector connecting them (10).

In further keeping with the molecular exciton hypothesis, heating of TMR–5′-TARm-3′–DABCYL to 65°C, a temperature well above the 42 ± 1°C melting temperature, restores the absorption spectrum to one close to that of the mixture of singly labeled TARm species (Fig. 2A). This confirms that the absorption changes in the molecular beacon reflect the spatial proximity of the two dyes. The emission spectrum of TMR–5′-TARm-3′–DABCYL showed 93% fluorescence quenching as compared with the mixture of the two singly labeled sequences (Table 1). In contrast, no shift in the emission maximum is observable (Fig. 2B) and the fluorescence decay of TMR–5′-TARm-3′–DABCYL is indistinguishable from that of TMR–5′-TARm (Table 1). Moreover, the excitation spectrum of TMR–5′-TARm-3′–DABCYL clearly differs from its absorption spectrum but closely resembles the absorption spectrum of TMR–5′-TARm (Fig. 2B). Taken together, our data confirm that the molecular beacon is essentially non-fluorescent (1). The residual fluorescence of TMR–5′-TARm-3′–DABCYL

Table 1. Absorption and emission properties of the singly and doubly labeled oligonucleotides investigated in the present study

	λ_{P1} (nm)[a]	λ_{P2} (nm)[a]	A_{P1}/A_{P2}[a]	Q (%)[b]	τ_1 (ns)[c]	α_1 (%)[c]	τ_2 (ns)[c]
TMR–5′-TARm	559			0	2.9 ± 0.2	52 ± 6	0.8 ± 0.2
TMR–5′-TARm-3′–TMR	558	520	0.70	80	2.9 ± 0.2	65 ± 8	0.5 ± 0.1
TMR–5′-TARm-3′–DABCYL	562	486	1.53	93	3.1 ± 0.7	55 ± 9	0.6 ± 0.3
DABCYL–5′-TARm-3′–TMR	563	486	1.26	86	3.6 ± 0.3	50 ± 9	0.9 ± 0.3
TMR–5′-K1-3′–DABCYL	563	492.5	1.40	86	4.5 ± 0.4	35 ± 5	1.0 ± 0.2
TMR–5′-K2-3′–DABCYL	562	492.5	1.40	80	3.8 ± 0.4	65 ± 8	0.9 ± 0.2
TMR–5′-TARm(–*i*)-3′–DABCYL	558	482	1.56	75			
Rh6G–5′-TARm-3′–DABCYL	535	480	0.90	95			

[a]λ_{P1} and λ_{P2} designate the wavelengths of the two absorbance peaks of the doubly labeled oligonucleotides. A_{P1}/A_{P2} corresponds to the absorbance ratio of these two peaks.
[b]The extent of TMR or Rh6G fluorescence quenching (Q) was obtained by comparing the fluorescence of a given doubly labeled oligonucleotide with that of the corresponding oligonucleotide singly labeled with TMR or Rh6G.
[c]The fluorescence lifetimes and their corresponding amplitudes were expressed as means (± SEM) for three independent measurements. The presence of two lifetimes is usual in TMR-labeled oligonucleotides and has been attributed to the coexistence of two states that differ by the proximity between TMR and a guanosine-rich area (26).

may be due to species with the two dyes not close together or contamination from singly labeled TMR–5′-TARm species.

Spectral characteristics of a homodoubly end-labeled TARm sequence

Since intramolecular excitonic homodimers lead to more easily interpretable spectra than heterodimers, a homodoubly labeled TMR–5′-TARm-3′–TMR sequence with TMR dyes at both the 5′- and 3′-ends was used. The absorption spectrum of this derivative revealed large spectral changes as compared with an equimolar mixture of TMR–5′-TARm and TARm-3′–TMR (Fig. 3A). The major feature is the appearance of a blue shifted peak at 520 nm, which disappears with heating. Exciton theory predicts that the doubly degenerate excited energy level in a system of two non-interacting monomers splits into two upon dimerization. If transitions to both excited levels were allowed, two absorption peaks positioned at both sides of the major absorption peak (at 558 nm) of the monomer would be expected. In contrast, the presence of only a blue shifted peak is indicative of an H-type geometry. As in TMR, the transition dipole corresponding to the visible band is oriented along the nitrogen–nitrogen axis (24) it results that the two dyes may be either stacked on each other or aligned side-by-side. These two arrangements can in theory be discriminated by the spectral shifts of the absorption band in the near UV range (~350 nm) whose transition dipole is perpendicular to that of the visible band. Unfortunately, the absence of this band in TMR–5′-TARm-3′–TMR precluded definitive discrimination between the two arrangements.

The emission spectrum of TMR–5′-TARm-3′–TMR resembles that of a mixture of the two singly-labeled sequences but is quenched by 80% (Table 1). This extent of fluorescence quenching was slightly lower than in TMR–5′-TARm-3′–DABCYL. Mass spectrometry indicated that this was not linked to the presence of a larger amount of singly labeled TARm molecules (data not shown). Moreover, low structural stability or improper folding of TMR–5′-TARm-3′–TMR could also be excluded since addition of 5 mM Mg^{2+}, lowering of the temperature to 10°C or a denaturation–renaturation

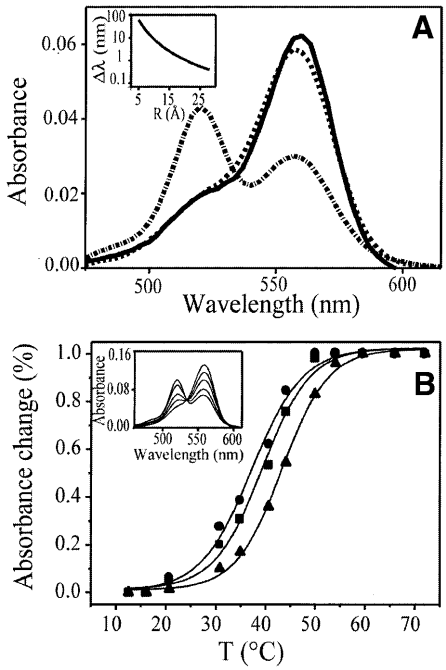

Figure 3. Spectral properties and melting curves of TMR–5′-TARm-3′–TMR. (**A**) Absorption spectra of TMR–5′-TARm-3′–TMR at 20 (dash-dotted line) and 65°C (dashed line). The solid line corresponds to the absorption spectrum of an equimolecular mixture of TMR–5′-TARm and TARm-3′–TMR. The insert shows the dependence of the wavelength shift of the blue shifted peak (which results from exciton splitting) on the interchromophore distance. The orientation between the dyes is assumed to be constant. (**B**) Melting curve of TMR–5′-TARm-3′–TMR. The relative absorbance changes were recorded at 260 (triangle), 521 (square) and 558 nm (circle). The experimental points were fitted to equation **1**. The insert shows, from top to bottom (with respect to the 558 nm peak), the absorption spectra recorded at 16, 31, 40.5, 44 and 60°C, respectively.

cycle did not change the extent of quenching (data not shown). Interestingly, differences in the extent of fluorescence quenching between different couples of dyes have also been reported for doubly labeled protease substrates and attributed to the ability of the dyes to interact together (27).

In addition, the temperature dependence of the spectral properties of TMR–5′-TARm-3′–TMR was investigated. With increasing temperature a progressive decrease in absorbance of the blue shifted band and a simultaneous increase in absorbance of the main band of monomeric TMR were observed (Fig. 3B). The relative absorbance changes in both peaks were superimposable, confirming that they describe the same mechanism. Both curves were shifted by ~4°C towards low temperatures with respect to the absorbance changes at 260 nm that report melting of the stem. Accordingly, it appears that disappearance of the exciton band precedes melting of the stem. Similar results were obtained when TMR–5′-TARm-3′–TMR was substituted by TMR–5′-TARm-3′–DABCYL (data not shown).

Dependence of exciton interaction on the oligonucleotide sequence and the dyes

As a first step we investigated the dependence of exciton interaction on the respective position of the two chromophores using DABCYL–5′-TARm-3′–TMR, in which the two dyes were inverted with respect to TMR–5′-TARm-3′–DABCYL. The large changes in the absorption spectrum of DABCYL–5′-TARm-3′–TMR at 20 as compared with 65°C indicated that an exciton interaction also takes places in this derivative. The position of the two absorption peaks (Table 1) was as in TMR–5′-TARm-3′–DABCYL but the peak absorbance ratio and the extent of fluorescence quenching were slightly different, suggesting limited differences in the orientation and magnitude of the transition dipoles in the two derivatives.

In a second step we tested the dependence of exciton interaction on the nucleic acid sequence using two 28mer oligonucleotides, K1 and K2, which differ in sequence from TARm (Fig. 1). These sequences form hairpins with an 8 bp stem and are thus representative of the usual sequences in molecular beacons. While the loops are the same in K1 and K2, the stems are inverted. Thus the chromophores are linked to a C-G pair in K1 and an A-T pair in K2. The exciton interactions in TMR–5′-K1-3′–DABCYL and TMR–5′-K2-3′–DABCYL were determined by comparison of the absorption spectra at 20 and 65°C (Fig. 4A). The spectral properties of these two derivatives were very similar and differed from those of TMR–5′-TARm-3′–DABCYL by a slightly lower peak absorbance ratio and spectral shift. Accordingly, the stem sequence and length may modulate to some extent the exciton interaction. In keeping with the dependence of TMR fluorescence parameters on the oligonucleotide sequence (26,28), significant differences were observed for the lifetimes and associated amplitudes of TMR in the various derivatives.

In a next step we investigated the spectral properties of TMR–5′-TARm(–*i*)-3′–DABCYL derivatives, where the 3′-terminal end of TARm was shortened by i = 1–3 nt. The absorption spectra of the three shortened derivatives were remarkably similar to that of the full-length derivative and were thus indicative of an exciton interaction. Hence, the $(CH_2)_6$-NH- and $(CH_2\text{-}CH_2\text{-}O)_3\text{-}(CH_2)_2$-NH- arms linking TMR and DABCYL, respectively, to the stem (Fig. 1B) are of sufficient length and flexibility to allow formation of an intramolecular ground state heterodimer, which should be energetically favorable.

Since DABCYL can be associated with various fluorophores in molecular beacons, we investigated the effect of substituting

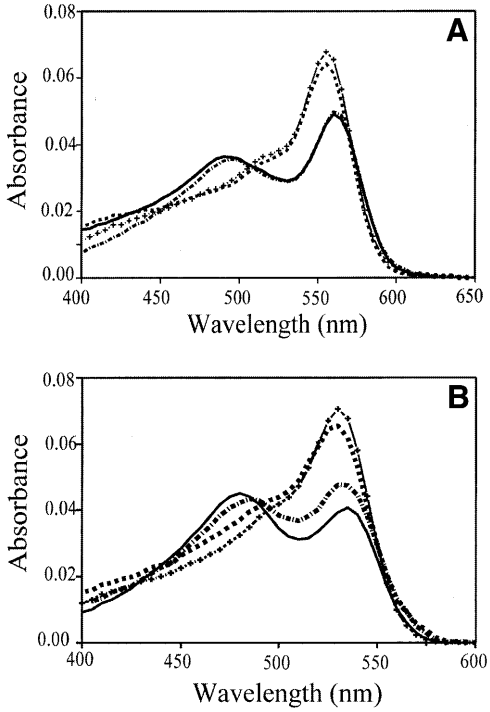

Figure 4. Dependence of exciton interaction on the oligonucleotide and xanthene dye. (**A**) Absorption spectra of TMR–5′-K1-3′–DABCYL at 20 (solid line) and 65°C (dashed line) and of TMR–5′-K2-3′–DABCYL at 20 (dash-dotted line) and 65°C (crosses). The melting temperature of both oligonucleotides is 54°C. (**B**) Absorption spectra of Rh6G–5′-TARm-3′–DABCYL at 20 (solid line) and 65°C (crosses) and of the RNA analog of Rh6G–5′-TARm-3′–DABCYL at 20 (dash-dotted line) and 65°C (dashed line).

TMR with Rh6G, whose major absorption band is at 533 nm. Exciton interaction in Rh6G–5′-TARm-3′–DABCYL could be readily inferred from the temperature-dependent spectral changes in Figure 4B. These changes were even larger than in TMR–5′-TARm-3′–DABCYL, but the extent of fluorescence quenching was similar (Table 1). In addition, the spectral properties of Rh6G–5′-TARm-3′–DABCYL were not altered when the deoxyribonucleic sequence was substituted by its RNA analog (Fig. 4B). This suggested that the nature of the nucleic acid does not strongly affect the exciton interaction.

Use of exciton interaction in nucleic acid hybridization

The hybridization of an oligonucleotide with its complementary sequence was followed by two different protocols based on exciton interaction. In the first protocol a mixture of TMR–5′-TARm-3′–DABCYL with its complementary unlabeled sequence, TARc, was heated to 85°C and then stepwise cooled. This induced total disappearance of the exciton band and restored an absorption spectrum (Fig. 5) similar to that of an equimolecular mixture of TMR–5′-TARm and TARm-3′–DABCYL (Fig. 2A). In contrast, the exciton band was unaffected when TMR–5′-TARm-3′–DABCYL was mixed with a non-complementary sequence. The second protocol was based on formation of intermolecular excitonic dimers obtained by annealing TARm-3′–DABCYL with its complementary sequence, TMR–5′-TARc 5′-labeled with TMR. The experiment was performed in a two-compartment quartz cell. TARm-3′–DABCYL was introduced into the first compartment and the

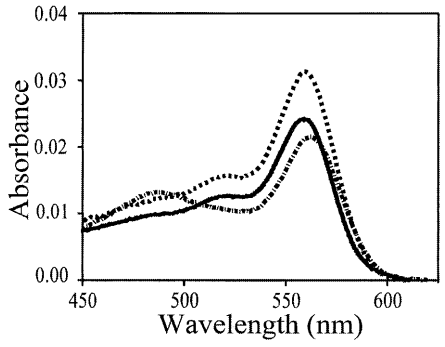

Figure 5. Use of exciton interaction to show nucleic acid hybridization. Absorption spectra of an equimolecular mixture of TMR–5′-TARc and TARm-3′–DABCYL at 20°C before (dashed line) and after (dash-dotted line) hybridization. The solid line corresponds to the absorption spectrum of TMR–5′-TARm-3′–DABCYL hybridized by temperature to its complementary unlabeled sequence TARc.

same concentration of TMR–5′-TARc was introduced into the second one. The absorption spectrum was first recorded at 20°C, in order to obtain the sum of the two spectra (Fig. 5). The contents of the compartments were then mixed, heated to 70°C and cooled to 20°C. This led to a spectrum highly similar to that of TMR–5′-TARm-3′–DABCYL, suggesting that an intermolecular excitonic dimer formed during the annealing process. Moreover, TMR fluorescence was quenched by ~90% during the annealing process, further suggesting that inter- and intramolecular excitonic dimers have similar spectral properties. In addition, as the final species in the annealing process is a doubly end-labeled duplex this suggests that the spectral properties of excitonic dimers may also be used to follow structural changes in duplexes.

DISCUSSION

In the present work an exciton interaction was demonstrated in molecular beacons and homodoubly end-labeled oligonucleotides. This interaction is associated with formation of ground state homo- or heterodimers with H-type geometry and leads to strong absorbance changes that disappear with melting of the stem. The formation of these H-type dimers partly depends on the forces holding the two chromophores together, since similar dimers form spontaneously in concentrated rhodamine solutions (29). Moreover, formation of ground state dimers was found to be poorly sensitive to the stem sequence, the respective position of the two dyes at the stem extremities, the nature of the xanthene dye and the nucleic acid (DNA or RNA), suggesting that the exciton interaction constitutes a common feature in molecular beacons. In addition, the exciton interaction is not limited to molecular beacons but operates with any double-stranded sequence and almost any pair of chromophores (manuscript in preparation).

Exciton interaction may also explain the very low fluorescence of molecular beacons, since in H-type dimers only transitions from the ground state to the exciton state of highest energy (corresponding to parallel transition dipoles between the chromophores) are allowed (30). After excitation a rapid internal conversion occurs and populates the lower excitation state, from which radiative transitions to the ground state are forbidden. It results in a radiationless intersystem crossing process and efficient triplet excitation.

The exciton interaction could be most easily discussed on the basis of the spectral properties of the homodoubly labeled TMR–5′-TARm-3′–TMR derivative. Simpson and Peterson (31) have classified the exciton interaction according to the value of the ratio $2\Delta\bar{\nu}/\Delta\varepsilon$, where $\Delta\bar{\nu}$ and $\Delta\varepsilon$ designate the absorption spectral shift and the Franck–Condon bandwidth, respectively. When this ratio is >>1 the strong coupling exciton case applies, whereas a ratio <<1 designates a weak coupling exciton case. Since in our derivative $\Delta\bar{\nu} = 1310\ cm^{-1}$ and $\Delta\varepsilon = 1150\ cm^{-1}$, the strong coupling conditions are not absolutely satisfied. Nevertheless, the formalism elaborated in the strong coupling case has also been shown to operate in such limiting cases (12,24).

In the absence of direct interchromophore orbital overlap the transition dipoles of the two chromophores are thought to interact via a long range Coulombic mechanism (12). Accordingly, for a strongly electric dipole-allowed transition, such as the visible band in TMR, the interaction energy ($U = hc\Delta\bar{\nu}$, where h and c designate the Planck constant and speed of light, respectively) may be adequately approximated by:

$$U = (1/4\pi\varepsilon_0) \times [\mu^2/(n^2 \times R^3)] \times \kappa \qquad \mathbf{2}$$

where R is the distance between the point dipole systems, ε_0 is the vacuum permittivity, μ^2 is the squared module of the transition dipole, n is the solvent refractive index ($n = 1.333$ in water) and κ is the orientation factor ($\kappa = 1$ for an H-type geometry) (24). The squared module of the transition dipole, expressed in $C^2\ m^2$, is calculated by:

$$\mu^2 = 1.02 \times 10^{-61} \int [\varepsilon(\bar{\nu})/\bar{\nu}] d\bar{\nu} \qquad \mathbf{3}$$

where $\varepsilon(\bar{\nu})$ corresponds to the extinction coefficient of TMR at a given wavenumber and the integral for the lowest energy transition of TMR is calculated from the absorption band in the visible range. A value of $9.5 \times 10^{-58}\ C^2\ m^2$ was obtained for μ^2, which allowed us to calculate an interdipole distance R of 5.7 Å. As this distance is in the range of the TMR dimensions, short range interactions, such as a two electron exchange interaction, and penetration effects may no longer be negligible (12). However, since in naphthalene these short range interactions have been shown to be small compared with the dipole–dipole interaction at interchromophore separations >5 Å (12), our calculated distance is thought to be a reasonable approximation.

If we assume that the chromophore orientation is kept constant, it can be deduced from equation **2** that the wavelength shift $\Delta\lambda$ (nm) of the blue shifted peak resulting from exciton splitting is extremely sensitive to the interchromophore distance (Fig. 3A, insert). Indeed, $\Delta\lambda$ decreases to <1 nm and is thus negligible for distances >20 Å. In fact, this limit is certainly overestimated, since the interchromophore forces (hydrogen and hydrophobic bonds) (29) will probably keep the TMR dyes together within a much shorter distance. This is illustrated by the melting curves of TMR–5′-TARm-3′–TMR. Disappearance of the exciton interaction precedes melting of the stem by 4°C, suggesting that unzipping starts either at or close to the 5′- and 3′-ends of the stem and that only partial melting of the stem (and thus a limited increase in the distance between the two dyes) is required for loss of the exciton interaction. Moreover, the identity of the relative absorbance

changes of the two peaks and the presence of a clear isosbestic point at 534 nm (Fig. 3B) strongly suggest that melting of the oligonucleotide follows a two-state model with regard to exciton interaction (32). In other words, no intermediate homodimer (which would be associated with a different absorption spectrum) with a different distance between and/or geometry of the dyes can be seen to accumulate during the melting process. The all-or-none behavior of the exciton interaction during the melting process can be related to dissociation of the ground state dimer, since an exact quantum mechanical resonance is required for the exciton interaction to operate (11). Indeed, it has been reported that this exact resonance is lost owing to environmental perturbation when the dyes no longer form a structured dimer but can be assimilated as a colliding pair of molecules (11). Accordingly, the absorbance changes that accompany formation of ground state dimers may be used as an extremely sensitive sensor to monitor short range modifications in the stem.

Since FRET requires a very weak dipolar coupling between the donor and acceptor (8–10), FRET measurements cannot be performed in the distance range where an exciton interaction occurs. The lower limit for FRET will depend on the chromophore and notably on its μ^2 value. It will also depend on the Förster critical distance R_0, since reliable distance measurements by FRET require that the distance is within a factor of 2 of R_0 (33). In the case of TMR–5′-TARm-3′–TMR and TMR–5′-TARm-3′–DABCYL the shortest distance is essentially related to R_0 values of 44 and 26 Å, respectively, which will preclude reliable distance measurements below 22 and 13 Å. This conclusion could be extended to most pairs of chromophores used in FRET since the R_0 values are generally between 22 and 75 Å (34). It thus appears that exciton coupling and FRET are complementary, allowing the investigation of non-overlapping distance ranges with the same pair of chromophores. Accordingly, the application of molecular beacons (and doubly end-labeled double-stranded oligonucleotides in general) can be extended to monitoring short range modifications of nucleic acid structure. This may be useful, for instance, in following the early events of stem or duplex unzipping or the mode of action of physical or chemical agents that induce incomplete unzipping. In this respect, experiments are in progress to investigate the mechanism of action of the nucleocapsid protein of HIV-1, which is thought to destabilize but not unwind DNA (35). Finally, in contrast to the spectral shifts, the relative absorbances of the two peaks of the exciton band were found to vary with various parameters. This points to subtle changes in the value or the orientation of the dipole transition moments. Efforts should be made to further develop the theoretical bases of these absorbance changes in order to obtain additional molecular information on the system.

ACKNOWLEDGEMENTS

We thank N. Potier and A. van Dorssaeler for performing mass spectrometry measurements, H. Lami for critical reading of the paper, J. A. Bousquet for discussions and N. Srividya for stylistic revision. This work was supported by grants from the Agence Nationale de Recherches sur le SIDA (ANRS), Sidaction (Ensemble contre le SIDA), Centre National de la Recherche Scientifique (programme PCV) and Université Louis Pasteur. S.B. was an ANRS fellow.

REFERENCES

1. Tyagi,S. and Kramer,F.R. (1996) Molecular beacons: probes that fluoresce upon hybridization. *Nat. Biotechnol.*, **14**, 303–308.
2. Leone,G., van Schijndel,H., van Gemen,B., Kramer,F.R. and Schoen,C.D. (1998) Molecular beacon probes combined with amplification by NASBA enable homogeneous, real-time detection of RNA. *Nucleic Acids Res.*, **26**, 2150–2155.
3. Sokol,D.L., Zhang,X., Lu,P. and Gewirtz,A.M. (1998) Real time detection of DNA.RNA hybridization in living cells. *Proc. Natl Acad. Sci. USA*, **95**, 11538–11543.
4. Giesendorf,B.A., Vet,J.A., Tyagi,S., Mensink,E.J., Trijbels,F.J. and Blom,H.J. (1998) Molecular beacons: a new approach for semiautomated mutation analysis. *Clin. Chem.*, **44**, 482–486.
5. Fang,X., Liu,X., Schuster,S. and Tan,W. (1999) Designing a novel molecular beacon for surface-immobilized DNA hybridazation studies. *J. Am. Chem. Soc.*, **121**, 2921–2922.
6. Kostrikis,L.G., Tyagi,S., Mhlanga,M.M., Ho,D.D. and Kramer,F.R. (1998) Spectral genotyping of human alleles. *Science*, **279**, 1228–1229.
7. Li,J.J., Geyer,R. and Tan,W. (2000) Using molecular beacons as a sensitive fluorescence assay for enzymatic cleavage of single-stranded DNA. *Nucleic Acids Res.*, **28**, e52.
8. Förster,Th. (1960) *Comparative Effects of Radiation*. John Wiley & Sons, New York, NY, pp. 300–341.
9. Förster,Th. (1965) Delocalized excitation and excitation transfer. In Sinanoglu,O. (ed.), *Modern Quantum Chemistry*. Academic Press, New York, NY, Vol. III, pp. 93–137.
10. Kasha,M. (1963) Energy transfer mechanisms and the molecular exciton model for molecular aggregates. *Radiat. Res.*, **20**, 55–71.
11. Kasha,M. (1991) Energy transfer, charge transfer and proton transfer in molecular composite systems. *Basic Life Sci.*, **58**, 231–251.
12. Scholes,D.S. and Ghiggino,K.P. (1994) Electronic interactions and interchromophore excitation transfer. *J. Phys. Chem.*, **98**, 4580–4590.
13. Potier,N., Van Dorsselaer,A., Cordier,Y., Roch,O. and Bischoff,R. (1994) Negative electrospray ionization mass spectrometry of synthetic and chemically modified oligonucleotides. *Nucleic Acids Res.*, **22**, 3895–3903.
14. Cantor,C.R. and Schimmel,P.R. (1980) *Biophysical Chemistry*. W.H. Freeman and Co., San Francisco, CA.
15. Berlman,I.B. (1971) *Handbook of Fluorescence Spectra of Aromatic Molecules*. Academic Press, New York, NY.
16. Baudin,F., Marquet,R., Isel,C., Darlix,J.L., Ehresmann,B. and Ehresmann,C. (1993) Functional sites in the 5′ region of human immunodeficiency virus type 1 RNA form defined structural domains. *J. Mol. Biol.*, **229**, 382–397.
17. Dingwall,C., Ernberg,I., Gait,M.J., Green,S.M., Heaphy,S., Karn,J., Lowe,A.D., Singh,M., Skinner,M.A. and Valerio,R. (1989) Human immunodeficiency virus 1 tat protein binds trans-activation-responsive region (TAR) RNA *in vitro*. *Proc. Natl Acad. Sci. USA*, **86**, 6925–6929.
18. Peterlin,B.M., Luciw,P.A., Barr,P.J. and Walker,M.D. (1986) Elevated levels of mRNA can account for the trans-activation of human immunodeficiency virus. *Proc. Natl Acad. Sci. USA*, **83**, 9734–9738.
19. Rice,A.P. and Mathews,M.B. (1988) Transcriptional but not translational regulation of HIV-1 by the tat gene product. *Nature*, **332**, 551–553.
20. Helga-Maria,C., Hammarskjold,M.L. and Rekosh,D. (1999) An intact TAR element and cytoplasmic localization are necessary for efficient packaging of human immunodeficiency virus type 1 genomic RNA. *J. Virol.*, **73**, 4127–4135.
21. Kim,J.K., Palaniappan,C., Wu,W., Fay,P.J. and Bambara,R.A. (1997) Evidence for a unique mechanism of strand transfer from the transactivation response region of HIV-1. *J. Biol. Chem.*, **272**, 16769–16777.
22. Guo,J., Henderson,L.E., Bess,J., Kane,B. and Levin,J.G. (1997) Human immunodeficiency virus type 1 nucleocapsid protein promotes efficient strand transfer and specific viral DNA synthesis by inhibiting TAR-dependent self-priming from minus-strand strong-stop DNA. *J. Virol.*, **71**, 5178–5188.
23. Tan,W., Fang,X., Li,J. and Liu,X. (2000) Molecular beacons: a novel DNA probe for nucleic acid and protein studies. *Chemistry*, **6**, 1107–1111.
24. Packard,B.Z., Toptygin,D.D., Komoriya,A. and Brand,L. (1996) Profluorescent protease substrates: intramolecular dimers described by the exciton model. *Proc. Natl Acad. Sci. USA*, **93**, 11640–11645.
25. Packard,B.Z., Toptygin,D.D., Komoriya,A. and Brand,L. (1998) Intramolecular resonance dipole-dipole interactions in a profluorescent protease substrate. *J. Phys. Chem. B*, **102**, 752–758.

26. Edman,L., Mets,U. and Rigler,R. (1996) Conformational transitions monitored for single molecules in solution. *Proc. Natl Acad. Sci. USA*, **93**, 6710–6715.
27. Packard,B.Z., Komoriya,A., Toptygin,D.D. and Brand,L. (1997) Structural characteristics of fluorophores that form intramolecular H-type dimers in a protease substrate. *J. Phys. Chem. B*, **101**, 5070–5074.
28. Ying,L., Wallace,M.I., Balasubramanian,S. and Klenerman,D. (2000) Ratiometric analysis of single-molecule fluorescence resonance energy transfer using logical combinations of threshold criteria: a study of 12-mer DNA. *J. Phys. Chem. B*, **104**, 5171–5178.
29. Valdes-Aguilera,O. and Neckers,D.C. (1989) Aggregation phenomena in xanthene dyes. *Acc. Chem. Res.*, **22**, 171–177.
30. Kasha,M., Rawls,H.R. and Ashraf El-Bayoumi,M. (1965) The exciton model in molecular spectroscopy. *Pure Appl. Chem.*, **2**, 371–392.
31. Simpson,W.T. and Peterson,D.L. (1957) Coupling strength for resonance transfer of electronic energy in Van der Waals solids. *J. Chem. Phys.*, **26**, 588–593.
32. Cohen,M.D. and Fischer,E. (1962) Isosbestic points. *J. Chem. Soc.*, **2**, 3044–3052.
33. Lakowicz,J.R. (1999) *Principles of Fluorescence Spectroscopy*, 2nd Edn. Plenum Press, New York, NY.
34. Wu,P. and Brand,L. (1994) Resonance energy transfer: methods and applications. *Anal. Biochem.*, **218**, 1–13.
35. Johnson,P.E., Turner,R.B., Wu,Z.R., Hairston,L., Guo,J., Levin,J.G. and Summers,M.F. (2000) A mechanism for plus-strand transfer enhancement by the HIV-1 nucleocapsid protein during reverse transcription. *Biochemistry*, **39**, 9084–9091.